#### **Research Article**

Haider A. A. Al-Katib\* and Ali A. A. AL-Turaihi

# Effect of GFRP bar length on the flexural behavior of hybrid concrete beams strengthened with NSM bars

https://doi.org/10.1515/eng-2022-0538 received July 15, 2023; accepted September 23, 2023

**Abstract:** This project aims to investigate the effect of nearsurface-mounted glass fiber reinforced polymer (GFRP) bars strengthening on the flexural behavior of hybrid reinforced concrete beams. Seven beams were made; one of these specimens had no strengthening and is considered as a reference beam. The other models were strengthened using near-surface-mounted GFRP bars at the bottom of beams with different lengths (0.5, 0.75, and 1) of effective span beams and diameters (8 and 12 mm) of GFRP bars. The beam length was 2,200 mm with 150 mm width and 240 mm depth. The flexural reinforcement consists of 2  $\phi$ 12 steel bars at the tension zone and 2  $\varphi$ 12 at the compression zone for all beams. Furthermore, to resist shear forces, φ12 steel bars were used, distributed along the length of the beams spaced at 125 mm c/c; two-point loads on the beams with 500 mm between them were applied at the mid-span. The investigated characteristics were cracking and failure load, crack width, deflection, and failure patterns. By examining the models, it was found that there is an improvement in failure load range from 11.54 to 53.84% relative to the control.

**Keywords:** hybrid concrete, bar diameter, near surface, flexural strength, glass fiber reinforced polymer (GFRP) bars

# 1 Introduction

Although hybrid concrete is not a new idea, it has recently received wide attention due to its effectiveness in bearing

\* Corresponding author: Haider A. A. Al-Katib, Department of Civil Engineering, Engineering College/Kufa University, Najaf, Iraq, e-mail: hayder.alkatib@uokufa.edu.iq

Ali A. A. AL-Turaihi: Department of Civil Engineering, Engineering College/Kufa University, Najaf, Iraq, e-mail: alia.alturaihi@student.uokufa.edu.iq

load capacity and cost-effectiveness [1]. Hybrid concrete can be defined as incorporating more than one type of concrete to take advantage of the properties of each type [2].

Where the upper layer is cast with high-strength concrete, and the layer subjected to tensile (lower layer) is cast using ordinary concrete [3], thus overcoming the problem of brittle failure of the high-strength and durability of ordinary concrete [4]. To improve the tensile zone, strengthening can be used. The strengthening and protecting concrete structures mainly mean making modifications and treatment of the basic structural members to increase their bearing the loads imposed on them [5,6]. Concrete structures are strengthened for several reasons, including the functional change of the structure, errors during construction, improper design, and seismic retrofit [7].

Concrete structures can be strengthened using fiber-reinforced polymers (FRP) through several methods, such as externally bonded FRP reinforcement, which is considered a good and effective method in practice, but premature debonding was observed. There are other common methods such as near-surface mounted (NSM) [8]. This method is used to strengthen the members subjected to bending stress against tensile forces, as the surrounding concrete will provide protection from environmental and mechanical damage [9].

The NSM FRP rods are a propitious technology. In the early 1950s, the NSM steel rebar was used to strengthen the RC structures in Europe [10]. The benefits of using FRP compared to steel in NSM technology are higher resistance to corrosion. Because of the light weight of the FRP, its installation is easier and faster than steel, and the groove size was reduced due to the higher tensile strength and better corrosion resistance of FRP [11].

This method is applied by excavating grooves on the concrete surface, then the grooves are filled with epoxy paste halfway, after that the bars are put in the grooves and pressed to be surrounded by the epoxy. Then, the epoxy is added again, and the surface is leveled [12].

The failure mode of RC beams with NSM FRP or steel bars depends on different variables. The compressive strength of concrete and the amount of steel reinforcement in the tensile zone effect on the failure mode of the RC beams, where the failure changes from flexural to crushing of concrete [13]. There are two types of rupture failure either pull-out or peeling off. When the FRP or steel bars are longer than the length of the cracking span at an ultimate stage in the models, splitting of cracking concrete surrounding the grooves and sudden failure will be occurred in case of pull-out [14].

Peeling-off concrete occurs when the applied load causes cracks to reach the end of the NSM bars. Even this case is a sudden failure and as a result, the concrete covering the groove from the end of the bar peel-offs. Debonding is another common failure mode, which occurs in different ways [15]: bond failure at the bar–epoxy interface, epoxy–concrete interface, splitting of epoxy cover, concrete cover separation, and secondary debonding failure mechanisms [16].

After an extensive review of existing literature, it has been observed that there is a lack of research studies on the topic of strengthening hybrid reinforced concrete beams using glass fiber reinforced polymer (GFRP) of various lengths. In order to address this gap in the literature, the present study has been initiated with the objective of investigating and exploring the strengthening of hybrid beams using glass fiber. This research aims to find effective ways to strengthen the reinforced hybrid concrete beams in flexural by using NSM glass fiber bars (GFRP). The NSM strengthening technique was first introduced to overcome the debonding problems of externally bonded reinforcement.

# 2 Experimental work

#### 2.1 Models details

This study includes seven reinforced hybrid concrete beams which cast in two-layer, concrete with compressive strength (50 MPa) in the compression layer and normal strength with

compressive strength (25 MPa) in the tension zone. The first model was made without strengthening, while the other beams were divided into two groups. Group one and group two strengthened using NSM of GFRP bars using diameter (8 and 12 mm), respectively with different lengths (0.5, 0.75, and 1) of clear span, shown in Table 1. Each specimen consists of a total length of 2,200 mm and cross-section dimensions of 150 mm width and 240 mm height. The effective span was 2,000 mm. The flexural reinforcement of all beams consists of  $4\phi12$  steel bars. Furthermore, to prevent shear failure,  $\phi12$  steel bars were used, distributed along the length of the specimens spaced at 125 mm c/c as shown in Figure 1. Figure 2 shows the strengthening beams detail. Depending on ACI 318-19 [17], beams were designed to be failed in flexure failure.

The strengthening procedures began by cutting grooves with dimensions of about  $1.5~\rm db \times 1.5~\rm db$  [16] (where db is the diameter of the NSM reinforcement) into the concrete cover of specimens at the side or tension face of the beam, as shown in Figure 3. The grooves are made using a special concrete cutter. A hammer and a hand chisel were used to remove any remaining concrete lugs and to roughen the lower surface of the groove. The grooves were washed with water and dried by a high-pressure air jet. The details of a typical groove are shown in Figure 4.

In the NSM reinforcement technique, strengthening bars are placed gently into grooves that cut into the concrete cover of the RC beams. Then, they bonded using an epoxy adhesive groove filler. The grooves were half-filled with epoxy, and then, the GFRP bar was placed inside the groove and lightly pressed. This forced the epoxy to flow around the inserted GFRP bar. In addition, the required epoxy was used to fill the groove and level the surface. To ensure the epoxy achieved full strength, the beam was kept for 1 week as curing time.

## 2.2 Material properties

For all beams, ready-mixed concrete made of 19 mm max size of AL-Nibaae coarse aggregate, natural sand from Al-

Table 1: Details of beams

Name	Dim. Of GFRP	Length of GFRP	No. of NSM	Placement of NSM	Ratio of span
НВС			No		
HBD8L1	8 mm	1,000 mm	1	bottom	0.5 of span
HBD8L2	8 mm	1,500 mm	1	Bottom	0.75 of span
HBD8L3	8 mm	2,000 mm	1	Bottom	1 of span
HBD12L1	12 mm	1,000 mm	1	Bottom	0.5 of span
HBD12L2	12 mm	1,500 mm	1	Bottom	0.75 of span
HBD12L3	12 mm	2,000 mm	1	Bottom	1 of span

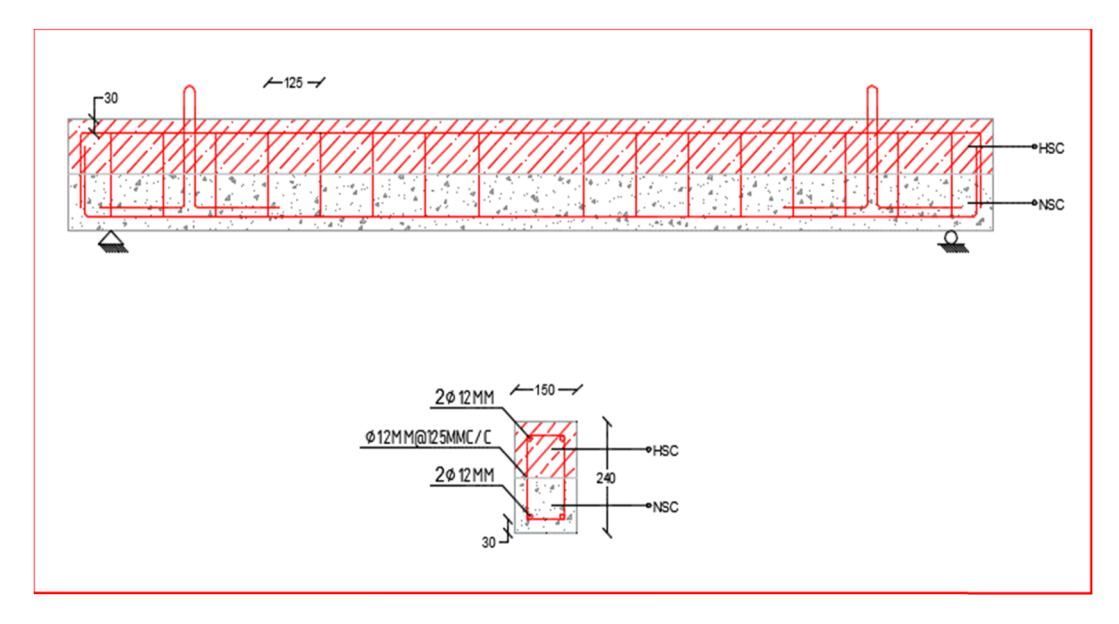


Figure 1: Details of tested beams.

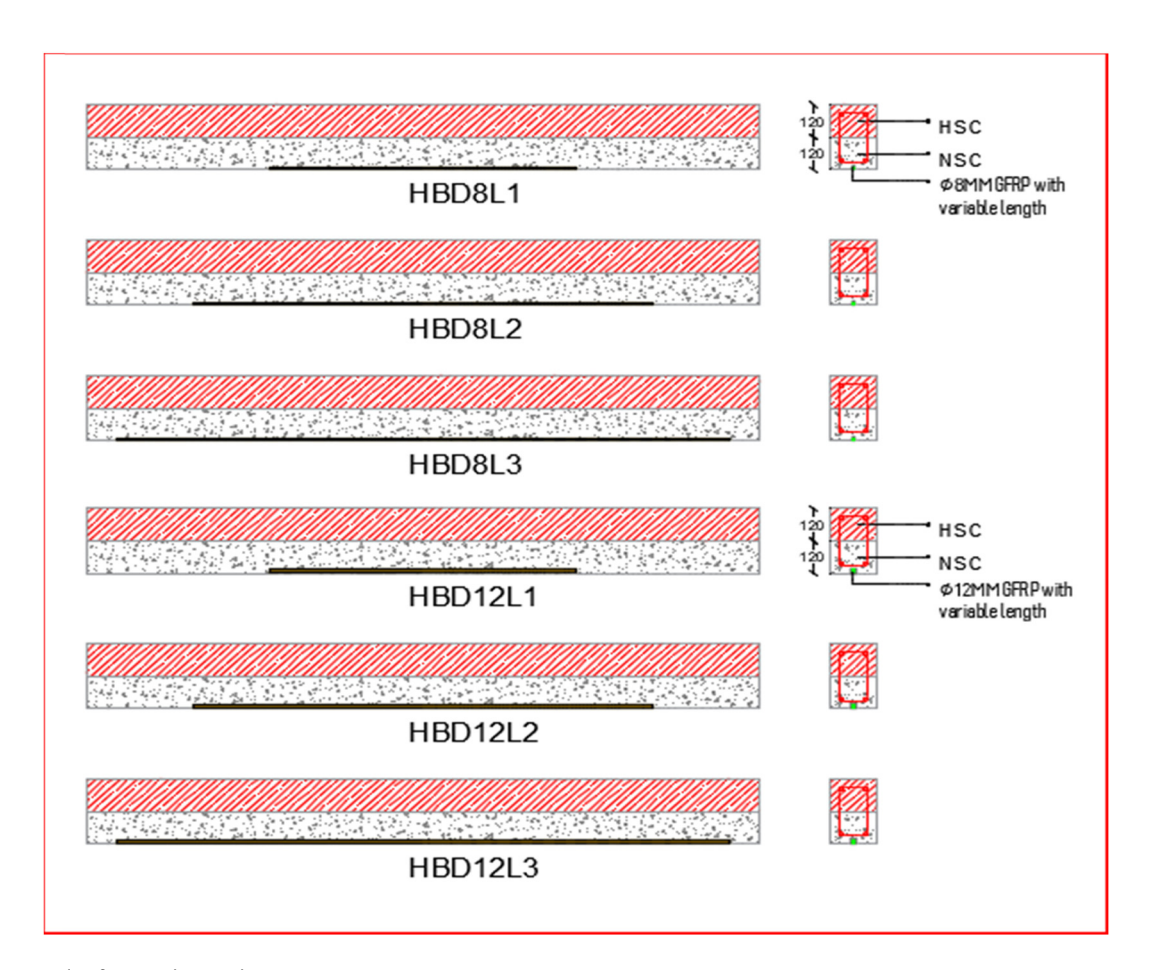


Figure 2: Details of strengthening beams.



Figure 3: Cut off the grooves.

Najaf region, AL-JESR Sulfur Resistant Portland cement, and tap water were used to prepare the concrete mix. In addition to silica fume (shown in Table 2) and Superplasticizer Concrete Admixture (Sika ViscoCrete-5930). Two types of concrete mixtures were made (chosen by trial mix) to obtain different compressive strengths as shown in Table 3.

The steel used as reinforcement was Rouhina steel;  $\varphi$ 12 steel bars were used as top and bottom longitudinal

reinforcements while  $\phi 12$  was used as shear (stirrup) reinforcement. The material properties of the steel reinforcement were measured using a hydraulic loading frame in the Civil Engineering, Structural Laboratory and listed in Table 4. The GFRP bar that was used in the NSM strengthening had a diameter of 8 and 12 mm. The material properties of the GFRP are listed in Table 5. Sikadur 30 was used to bond the GFRP bars in the bottom grooves of the beams, and the properties listed in Table 6.



Figure 4: Application of NSM bars.

Table 2: Silica fume properties

Physical properties	Surface area	Approximately 24,000–28,000 m <sup>2</sup> /kg
	Variation average fineness	Approximately 2% maximum
	Pozzolanic activity index (28 days)	Approximately 105% minimum
	Grading – below 1 μm	Minimum 90%
Chemical content	SiO <sub>2</sub>	Approximately 90% minimum
	SO <sub>3</sub>	Approximately 0.2% maximum
	CaO	Approximately 0.8% maximum
	Cl <sup>-</sup>	Approximately 0.035% maximum

Table 3: Components of concrete mix

Materials	Mix type A	Mix type B
Cement (kg)	500	350
Coarse aggregate (kg)	800	1,200
Fine aggregate (kg)	880	800
W/S	26%	42%
Superplasticizer (L/m³)	7.5	_
Silica fume (% of cement)	15	_

## 2.3 Experimental setup

The flexural tests were performed in the structural testing Laboratory of the Faculty of Engineering – Kufa University. The tested beams are simply supports, plates, and rollers put over the under points of loads and supports to prevent local concrete crushing. The supports are placed 100 mm from the ends of the models, and the effective span was 2,000 mm. Figure 5 shows the experimental test setup beam. To measure the deflection of each span of the beam, three dial gages were used at mid-span, 666 and 333 mm from support; 5 kN/min was the actuator rate. During the test, the beam crack width was measured using a crack meter.

## 3 Results and discussions

The test results obtained from the examination of seven samples and presented in Table 7. One of these models has no strengthening and is considered as a reference model. The other models were strengthened using near-surface mounted GFRP. Two parameters, diameter and length of bars, were

studied. It was observed from the test results that there is an increase in the failure load, an enhancement in the first crack load, and a reduction in the deflection for the strengthening models compared to the control beam.

#### 3.1 Load-deflection curve

The load-deflection curves for set one (HBD8L1, HBD8L2, HBD8L3) and set two (HBD12L1, HBD12L2, and HBD12L3) with the control beam HBC shown in Figures 6 and 7, respectively. In the first stage, all strengthening samples showed linear behavior up to the first crack. It was observed that

Table 5: GFRP material properties

Normal diameter (mm)	Elastic modules (MPa)	Ultimate strength (MPa)
8	50202.773	1131.3
12	53513.031	1,198

Table 6: Sikandar 30 properties

Compressive strength (MPa)	75
Modulus of elasticity in compression (MPa)	9,600
Tensile strength (MPa)	26
Tensile modulus of elasticity (MPa)	11,200
Shear strength (MPa)	16
Tensile adhesion strength (MPa)	Concrete >4 N/mm <sup>2</sup> *
	Steel >21 N/mm <sup>2</sup>

<sup>\*100%</sup> concrete failure.

Table 4: Steel bars properties

Normal diameter (mm)	Yield strength (MPa)	Ultimate strength (MPa)	Elongation %
12	525	697	16
ASTM A615M	>420 ok	>620 ok	>9 ok

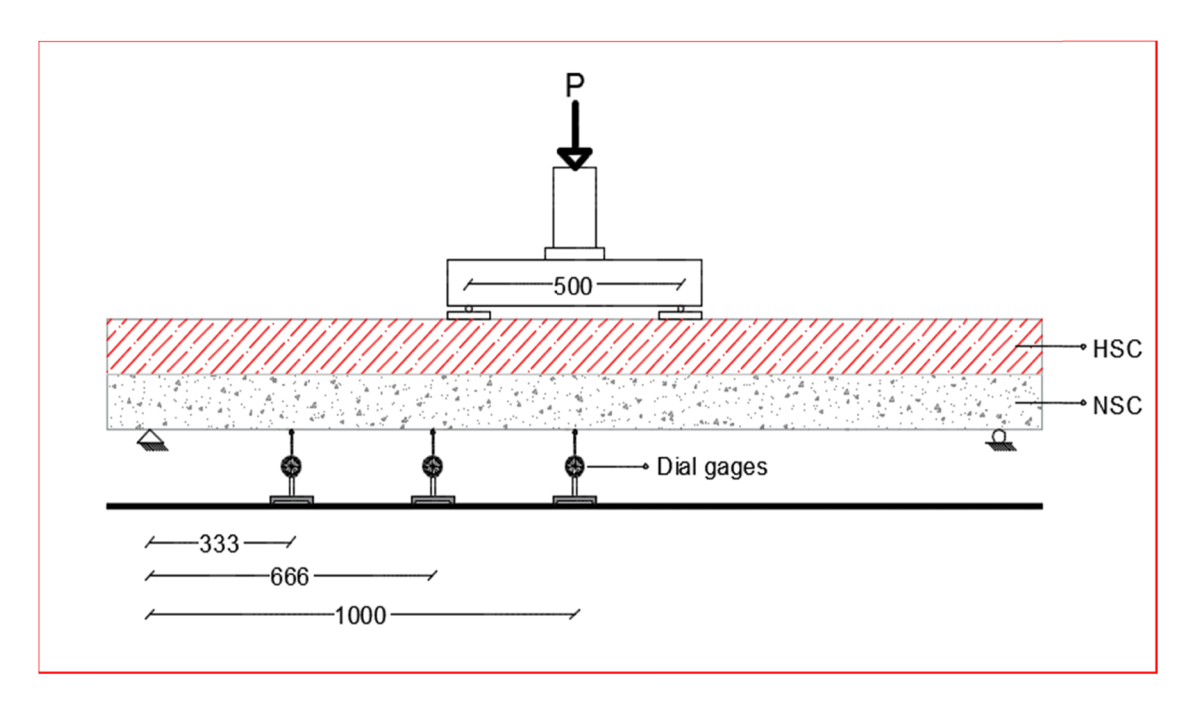


Figure 5: Experimental test setup beam.

Table 7: Tested beams results

	First crack load	Percentage of increase in first crack load %	Failure load	Percentage of increasing in failure load %	Deflection at failure (mm)	Crack width	Failure mode
НВС	15	_	78	_	25.73	2.17	Flexural failure
HBD8L1	25	66.66	87	11.538	20.76	1.68	Flexural failure
HBD8L2	25	66.66	90	15.384	21.23	1.17	Flexural failure
HBD8L3	25	66.66	98	25.641	27.47	1.98	Flexural failure
HBD12L1	25	66.66	90	15.384	16.73	0.75	concrete cover separation
HBD12L2	25	66.66	112	43.589	25.32	1.03	concrete cover separation
HBD12L3	25	66.66	120	53.846	26.5	1.15	Flexural failure

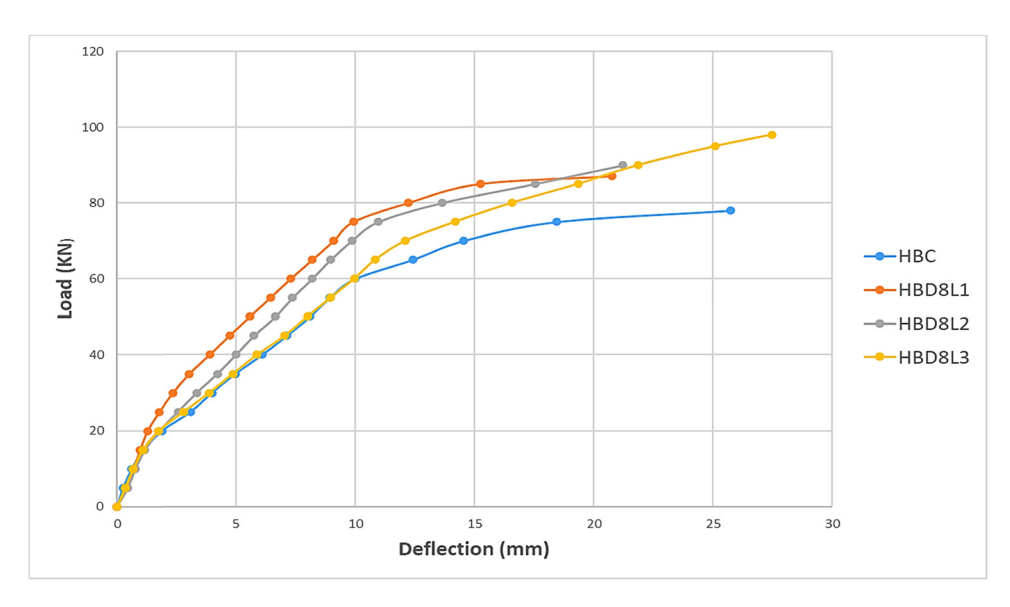


Figure 6: Load-deflection curves for (set 1).

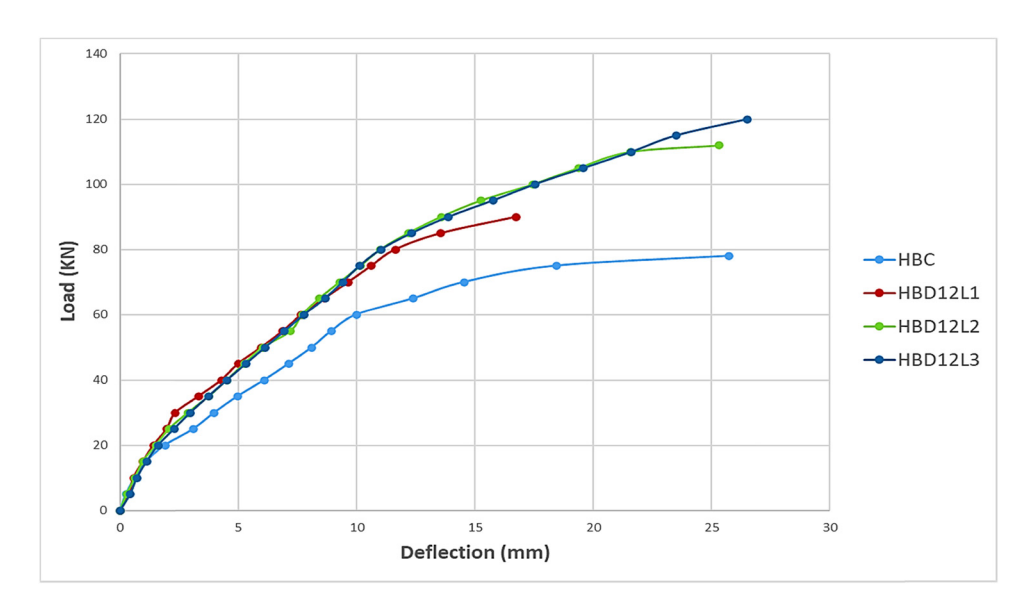


Figure 7: Load-deflection curves for (set 2).

there was an increase in the load of first cracking about 66.66% for all strengthening models compared with HBC. In the second stage, the behavior of curves was nonlinear until to failure point. The strengthening models showed more stiffness behavior compared to the control beam, This behavior was because the drilling in the models (HBD8L3, HBD12L2, and HBD12L2) exhausted the model, which made it less stiffness.

#### 3.2 Failure mode

Figure 8 presents the failure modes of beams tested in this research. The control model (HBC) failed flexural (as planned), as cracks appeared in the middle of the beam in the tensile zone, after which the cracks extended vertically to reach the compression zone. Nevertheless, the pattern of failure in group one was similar to HBC, but the



Figure 8: Failure mode of models.



Figure 9: Crack meter.

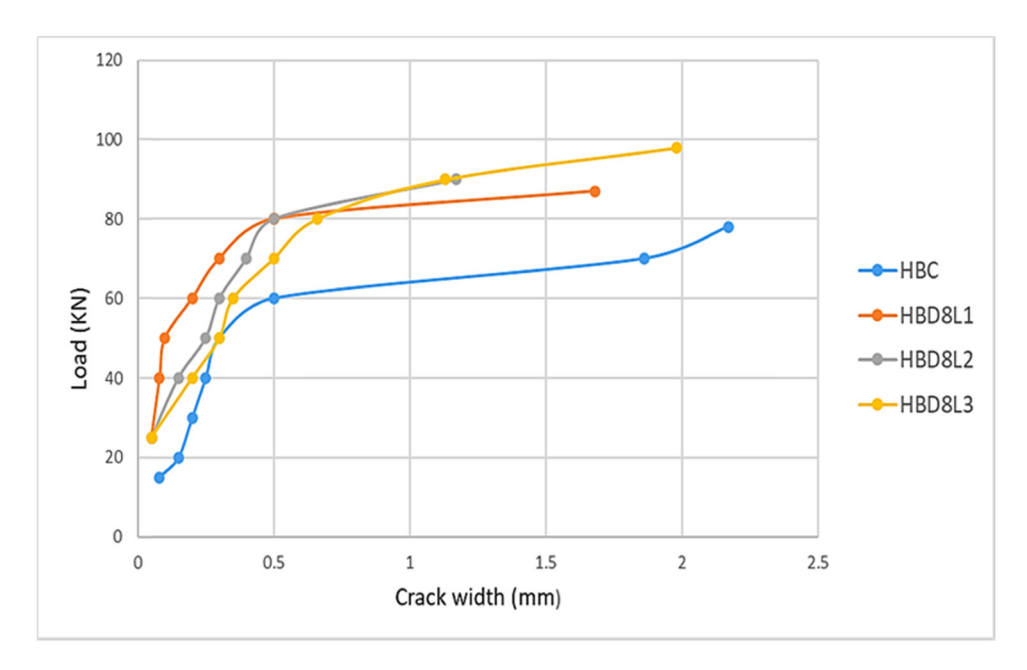


Figure 10: Load/maximum crack width for group one.

strengthening led to an increase in the failure load of about 11.538, 15.38, and 25.64% for HBD8L1, HBD8L2, and HBD8L3, respectively. Compared with HBC, it is noted in this group that the cracks increased before failure, with the appearance of flexural-shear cracks, which later turned into flexural. The increase in the failure load in HBD12L1, HBD12L2, and HBD12L3 of group two was 15.384, 43.589, and 53.846%, respectively, and failed by concrete cover separation for HBD12L1 and HBD12L2, where flexural-shear cracks appeared at the beginning, which later led to separation in the bottom

cover of the model, because the groove of the 12-diameter rod was wide led to weakening the cover area. While the beam HBD12L3 failed by flexural, the rod (2,000 mm) covered all the space of the model.

#### 3.3 Crack width

A crack meter (as shown in Figure 9) was used to measure the crack width of the beams. Figures 10–12 show the effect

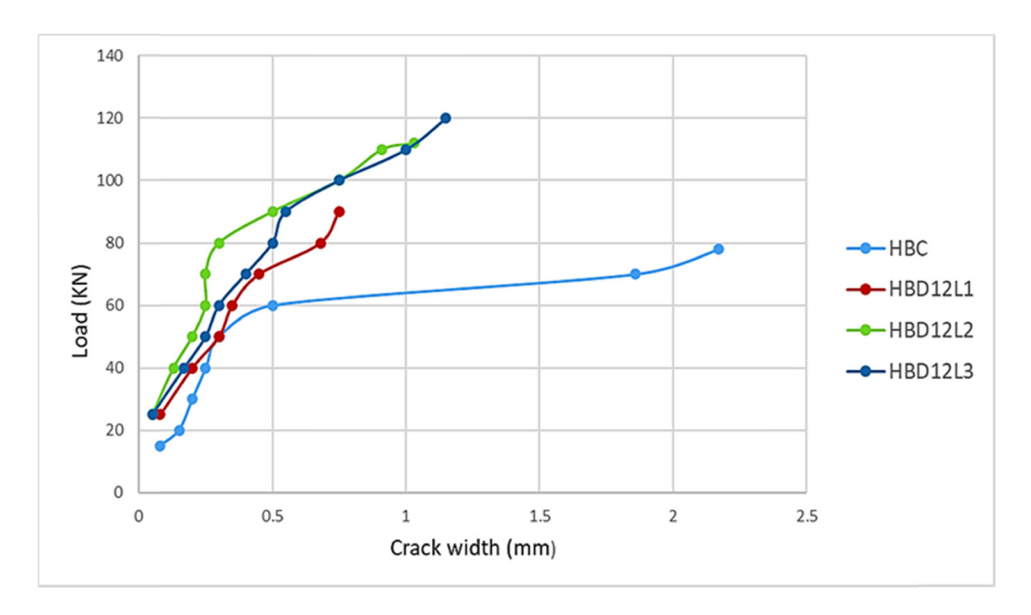


Figure 11: Load/maximum crack width for group two.

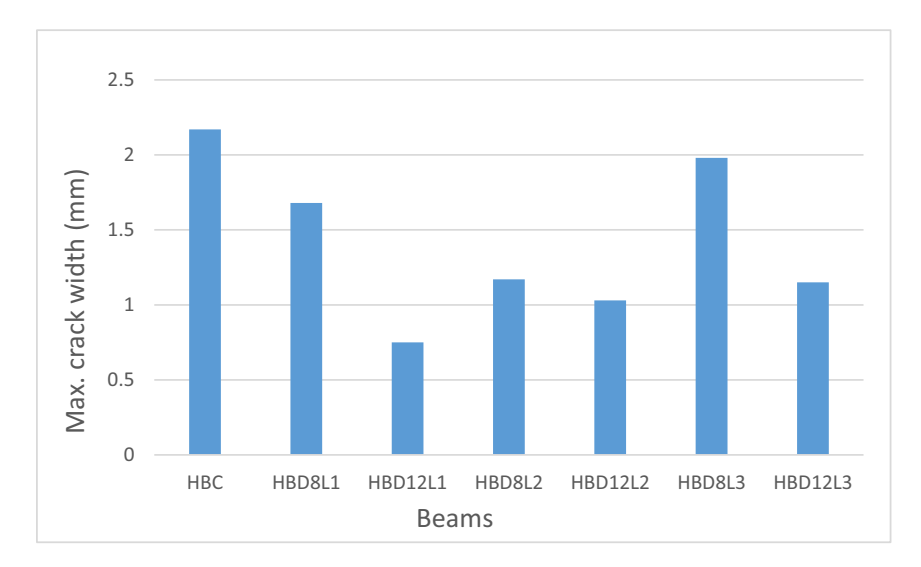


Figure 12: Maximum crack width for tested beam.

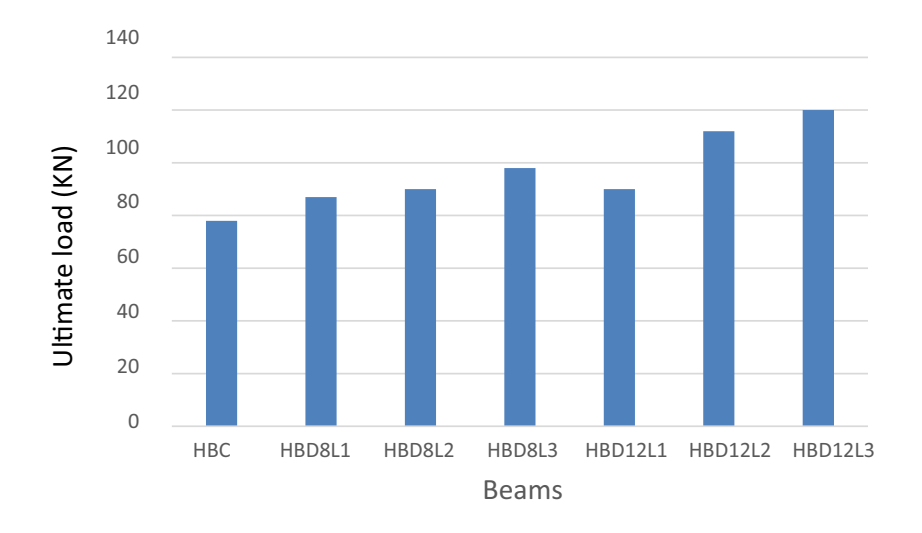


Figure 13: Ultimate load for tested beam.

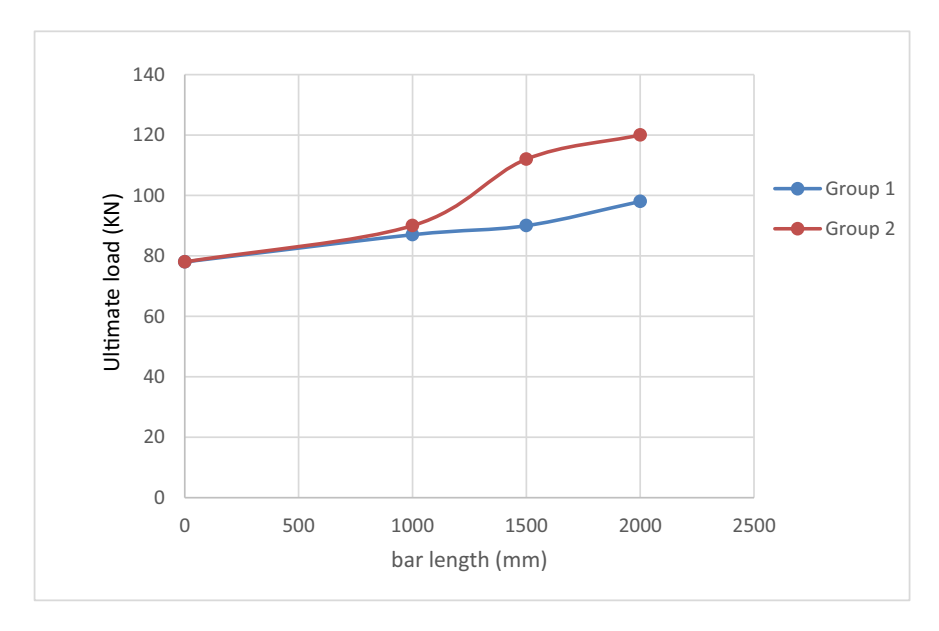


Figure 14: Ultimate load/bar length for groups one and two.

of the length and diameter of GFRP bars on the crack width.

It can be observed that the beams strengthening with the GFRP bar had lesser crack width as compared with NC beams. The diameter of the GFRP bar has the largest effect on the crack width. The crack width decreased as the diameter of GFRP bars increased. Due to the increase in the area of strengthening, the ability to impede the expansion of cracks increases.

# 4 Parametric study

# 4.1 Effect of NSM bars length

The bar lengths were changed to (0.5, 0.75, and 1) of clear span for group one (HBD8L1, HBD8L2, and HBD8L3), respectively, also group two (HBD12L1, HBD12L2, and HBD12L3) respectively. It was noted that an increase in the GFRP bar length led to an enhancement in failure load by 11.538, 15.38,

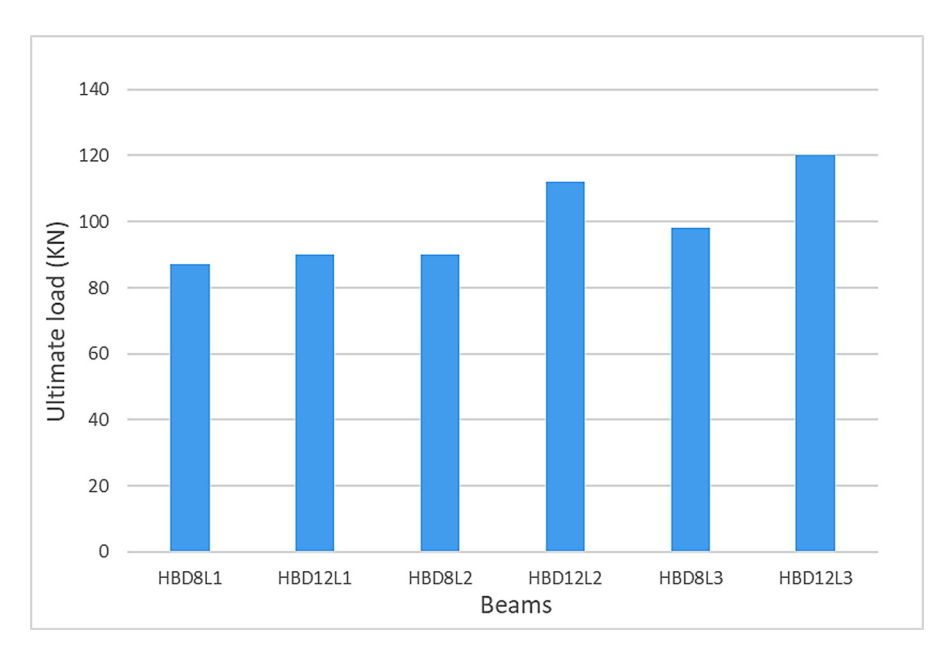


Figure 15: Ultimate load for tested beam.

and 25.64% for HBD8L1, HBD8L2, and HBD8L3, respectively, compared to HBC. While the failure load increased by 15.38, 43.59, and 53.84% for HBD12L1, HBD12L2, and HBD12L3, respectively, compared with HBC, the failure load in HBD12L1 increased by 3.44% compared with HBD8L1, 24.44% for HBD12L2 compared with HBD8L2, and 33.33% for HBD12L3 compared with HBD8L3, as shown in Figures 13 and 14. This increase is due to the efficiency of the rod diameter of 12 mm compared to the diameter of 8 mm.

#### 4.2 Effect of GFRP bar diameter

Figure 15 shows the GFRP bar diameter effect. The ultimate load was increased by about 3.448, 24.444, and 22.449% for HBD12L1, HBD12L2, and HBD12L3 compared with HBD8L1, HBD8L2, and HBD8L3, respectively.

# 5 Conclusion

In this research, the conclusion can be summarized in several points:

- 1. Strengthening the models by using the near-surface mounted technique led to a significant enhancement in the first crack and the failure load. The increase in the first cracking load was equal to 66.66% while the failure load was increased from 11.54 to 53.84% compared with the control beam.
- 2. The change in GFRP bar length and diameter had no effect on the first crack load.
- 3. The strengthening samples had more stiffness compared to the unstrengthening samples.
- 4. Strengthening by GFRP bar with a length equal to a clear span gives better results and prevents separation of the concrete cover since the strengthening crosses the flexural stresses region into the shear stresses region.
- 5. Increasing in length of GFRP bar did not lead to an increase in the stiffness of the beams.
- 6. The width of the crack decreases as the diameter of the GFRP bar increases, while the length of the GFRP bar did not affect the crack width.

**Acknowledgments:** The authors extend their thanks to all the staff in the structural laboratory of Kufa University.

**Author contribution:** All authors have accepted responsibility for the entire content of this manuscript and consented to its submission to the journal, reviewed all the results and approved the final version of the manuscript. AAAL-T carried out the experiment and wrote the manuscript while HAAA-K conceived the original idea and supervised the project.

Conflict of interest: Authors state no conflict of interest.

**Data availability statement:** Most datasets generated and analyzed in this study are in this submitted manuscript. The other datasets are available on reasonable request from the corresponding author with the attached information.

# References

- Abtan Y, Jaber H. Behavior of hybrid reinforced concrete beams combining reactive powder concrete and varying type of lightweight concrete. J Eng Sustain Dev. 2016;20(2):204–23.
- [2] Shami A, Al-Katib H. Shear Behavior of Isolated Hybrid concrete beam with Circular openings strengthening with CFRP. J Hunan Univ (Nat Sci). 2022;49(6):17.
- [3] Makki R, Alalikhan A, Al-katib H. Load-deflection behaviour of hybrid concrete flat slab. Eng Environ Sci. 2019;28(4):516–25.
- [4] Khalifa A. Flexural performance of RC beams strengthened with near surface mounted CFRP strips. Alex Eng J. 2016;55(2):1497–505.
- [5] Hosen M, Jumaat M, Saiful Islam A. Inclusion of CFRP-epoxy composite for end anchorage in NSM-epoxy strengthened beams. Adv Mater Sci Eng. 2015;2015:812797.
- [6] Hassan T, Rizkalla S. Investigation of bond in concrete structures strengthened with near surface mounted carbon fiber reinforced polymer strips. J Compos Constr. 2003;7(3):248–57.
- [7] Triantafillou T. Seismic retrofitting of structures with fibre reinforced polymers. Prog Struct Eng Mater. 2001;3(1):57–65.
- [8] Mahfuz K, Jumaat M, Shukri A, Obaydullah M, Huda M, Hosen M, et al. Strengthening of RC beams using externally bonded reinforcement combined with near-surface mounted technique. Polymers. 2016;8(7):261.
- [9] Panahi M, Izadinia M. A parametric study on the flexural strengthening of reinforced concrete beams with near surface mounted FRP bars. Civ Eng J. 2018;4(8):1917–29.
- [10] Nilimaa J, Blanksvärd T, Sas G. Flexural-shear failure of a full-scale tested RC bridge strengthened with NSM CFRP. 5th International conference on structural health monitoring of intelligent infrastructure (SHMII-5). 2011;11–5. December 2011, Cancún, México
- [11] Lorenzis L, Nanni A. Bond between near surface mounted FRP rods and concrete in structural strengthening. ACI Struct J. 2002;99(2):123–33.
- [12] Abdzaid H, Kamonna H. Flexural strengthening of continuous reinforced concrete beams with near-surface-mounted reinforcement. Pract Period Struct Des Constr. 2019;24(3):1–10.
- [13] Sharaky I, Torres L, Comas J, Barris C. Flexural response of reinforced concrete (RC) beams strengthened with near surface mounted (NSM) fibre reinforced polymer (FRP) bar. Compos Struct. 2014;109:8–22.
- [14] Lorenzis L, Nanni A, Tegola A. Flexural and shear strengthening of reinforced concrete structures with near surface mounted FRP rods. ACI Struct J. 2000;98(1):521–8.
- [15] Al-Mahmoud F, Castel A, François R, Tourneur C. Strengthening of RC members with near-surface mounted CFRP rods. Compos Struct. 2009;91(2):138–47.
- [16] Lorenzis L, Teng J. Near-surface mounted FRP reinforcement: An emerging technique for strengthening structures. J Compos Part B Eng. 2007;38(2):119–43.
- [17] ACI Committee 318. Building Code Requirements for Structural Concrete (ACI 318M-19) and Commentary (318RM-19). American Concrete Institute: Detroit, MI, USA; 2019.